J|A|C|S
ARTICLES
Published on Web 01/18/2003

Synthesis of Poly(6-azulenylethynyl)benzene Derivatives as a Multielectron Redox System with Liquid Crystalline Behavior

Shunji Ito,*,† Haruki Inabe,† Noboru Morita,† Kazuchika Ohta,‡ Teruo Kitamura,§ and Kimiaki Imafuku||

Contribution from the Department of Chemistry, Graduate School of Science, Tohoku University, Sendai 980-8578, Japan, Department of Functional Polymer Science, Faculty of Textile Science and Technology, Shinshu University, Ueda 386-8567, Japan, Fukuoka Industry, Science & Technology Foundation, Fukuoka Industrial Technology Center, Chikushino 818-8540, Japan, and Department of Chemistry, Faculty of Science, Kumamoto University, Kumamoto 860-8555, Japan

Received July 8, 2002; Revised Manuscript Received October 23, 2002; E-mail: ito@funorg.chem.tohoku.ac.jp

Abstract: A series of poly(6-azulenylethynyl)benzenes substituted with *n*-hexyloxycarbonyl chains at 1,3-positions in azulene rings, i.e., hexakis-, 1,2,4,5-tetrakis-, 1,3,5-tris-, and 1,4-bis(6-azulenylethynyl)benzene derivatives **1**, **2**, **3**, and **4b**, have been prepared by a simple one-pot reaction involving repeated Pd-catalyzed alkynylation of halogenated arenes with substituted 6-ethynylazulene and/or ethynylated arenes with substituted 6-bromoazulene under Sonogashira−Hagihara conditions. The redox behavior of these novel poly(6-azulenylethynyl)benzene derivatives was examined by cyclic voltammetry (CV), which revealed the presumed multielectron redox properties. Compound **4b** exhibited a one-step, two-electron reduction wave upon CV, which revealed the formation of the dianion stabilized by two 6-azulenylethynyl substituents under electrochemical reduction conditions. Four 6-azulenylethynyl substituents on a benzene ring in a 1,2,4,5 relationship increased the electron-accepting properties because of the formation of a stabilized closed-shell dianionic structure, whereas **3** was reduced at more negative reduction potentials. In contrast to the multistep redox behavior of **2**, compound **1** was reduced in one step at −1.28 V upon CV. Compound **1** showed a wide temperature range of columnar mesophases (Col_{ho} and Col_{ro}) from 77.3 °C to the decomposition temperature at ca. 270 °C. Compounds **2**, **3**, and **4b** exhibited columnar mesomorphism (Col_{ro}) with crystalline polymorphs for **2**, unusual triple-melting behavior for **3**, and both double-melting behavior and columnar mesomorphism (Col_{ho}) for **4b**. Therefore, the investigated systems exemplify a new principle for multielectron redox behavior with liquid crystalline properties.

Introduction

Electrochromism is observed in reversible redox systems, which exhibit significant color changes in different oxidation states.[1] Construction of organic molecules that contain multiple redox-active chromophores[2] is fairly important for the preparation of novel polyelectrochromic materials, which respond to different potentials with a variety of colors.[3] Hünig et al.[4] recently proposed a concept of a violene−cyanine hybrid to produce a stabilized organic electrochromic system. The hybrid is expected to provide a cyanine dye by an overall two-electron transfer as illustrated by the general structure in Scheme 1.

Recently, we have proposed that the redox system of unknown hexa(6-azulenyl)benzene is assumed as the hybrid in which the closed-shell cyanine-type structure would be also generated by the two-electron reduction (Chart 1).[5] Herein we point out the possibility for the construction of polyelectrochromic materials utilizing polyethynylbenzenes as a platform bearing multiple azulenes ($C_{10}H_8$) as redox-active chromophores. Hexakis(6-azulenylethynyl)benzene (**1**) should act as a three-step redox system, which will provide stabilized closed-shell dianion $\mathbf{1}_{red}^{-2}$, tetraanion $\mathbf{1}_{red}^{-4}$, and hexaanion $\mathbf{1}_{red}^{-6}$ by overall two-, four-, and six-electron transfers and could be expected to show significant change in the absorption spectra in the different oxidation states because the azulene system has a remarkable

* Corresponding author. Tel: +81-22-217-7714. Fax: +81-22-217-7714.
† Tohoku University.
‡ Shinshu University.
§ Fukuoka Industrial Technology Center.
|| Kumamoto University.

(1) Monk, P. M. S.; Mortimer, R. J.; Rosseinsky, D. R. *Electrochromism*: *Fundamentals and Applications*; VCH: Weinheim, Germany, 1995.
(2) Deuchert, K.; Hünig, S. *Angew. Chem., Int. Ed. Engl.* **1978**, *17*, 875−886.
(3) (a) Komatsu, T.; Ohta, K.; Fujimoto, T.; Yamamoto, I. *J. Mater. Chem.* **1994**, *4*, 533−536. (b) Rosseinsky, D. R.; Monk, D. M. S. *J. Appl. Electrochem.* **1994**, *24*, 1213−1221.
(4) (a) Hünig, S.; Kemmer, M.; Wenner, H.; Perepichka, I. F.; Bäuerle, P.; Emge, A.; Gescheid, G. *Chem. Eur. J.* **1999**, *5*, 1969−1973. (b) Hünig, S.; Kemmer, M.; Wenner, H.; Barbosa, F.; Gescheidt, G.; Perepichka, I. F.; Bäuerle, P.; Emge, A.; Peters, K. *Chem. Eur. J.* **2000**, *6*, 2618−2632. (c) Hünig, S.; Perepichka, I. F.; Kemmer, M.; Wenner, H.; Bäuerle, P.; Emge, A. *Tetrahedron* **2000**, *56*, 4203−4211. (d) Hünig, S.; Langels, A.; Schmittel, M.; Wenner, H.; Perepichka, I. F.; Peters, K. *Eur. J. Org. Chem.* **2001**, 1393−1399.
(5) (a) Ito, S.; Inabe, H.; Okujima, T.; Morita, N.; Watanabe, M.; Imafuku, K. *Tetrahedron Lett.* **2000**, *41*, 8343−8347. (b) Ito, S.; Inabe, H.; Okujima, T.; Morita, N.; Watanabe, M.; Nobuyuki, H.; Imafuku, K. *Tetrahedron Lett.* **2001**, *42*, 1085−1089. (c) Ito, S.; Inabe, H.; Okujima, T.; Morita, N.; Watanabe, M.; Nobuyuki, H.; Imafuku, K. *J. Org. Chem.* **2001**, *66*, 7090−7101.

10.1021/ja0209262 CCC: $25.00

Scheme 1

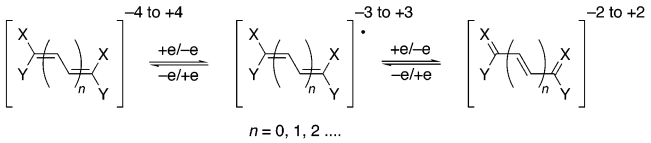

Chart 1

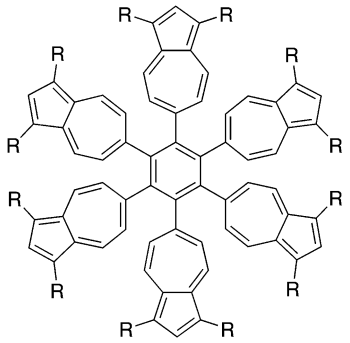

tendency to stabilize carbanions owing to its high polarizability (Chart 2).[6] The presumed cyanine-type structures formed by two- and four-electron reduction of **1** are represented by the bold line in Scheme 2.

We also report herein the successful synthesis of poly(6-azulenylethynyl)benzenes **2**−**4** for the comparison with the electrochemical properties of **1** (Chart 2). Compound **2** also could be assumed as a violene−cyanine hybrid in the point of the generation of a closed-shell cyanine-type structure by two-electron reduction. Compound **4** is a typical example for the general violene system and **3** exemplifies the redox system without conjugation in each azulenyl group.

Due to the hexyloxycarbonyl chains substituted at 1 and 3 positions on each azulenyl group, we anticipated these molecules would possess good solubility, fusibility, and the ability to self-organize in columnar mesophases.[7] The stacking behavior of discotic liquid crystals (LCs) provides opportunities for materials with one-dimensional transport processes such as energy migration, electric conductivity, and photoconductivity.[8] An EC-LC cell for laser beam writing is proposed for an application of the electrochromic materials with liquid crystalline properties.[9] We also report herein the liquid crystalline behaviors of **1**−**4**, which are the first examples exhibiting both multiple melting behavior and columnar mesomorphism in the chemistry of azulenes.

Results and Discussion

Synthesis. Poly(6-azulenylethynyl)benzenes **1**−**4** were prepared by a simple one-pot reaction involving repeated Pd-catalyzed alkynylation of halogenated arenes with substituted 6-ethynylazulene and/or ethynylated arenes with substituted 6-bromoazulene under Sonogashira−Hagihara conditions.[10,11] The preparation of diethyl 6-ethynylazulene-1,3-dicarboxylate (**5a**) was reported elsewhere.[5] Pd(0)-catalyzed reaction of **5a** with 1,4-diiodobenzene (**6**) afforded the desired bisadduct **4a**

Chart 2

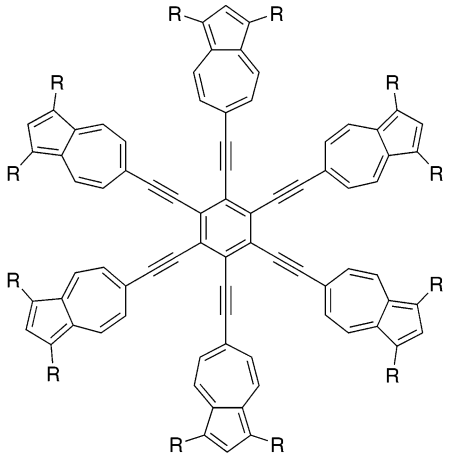

1: R = $COOC_6H_{13}$

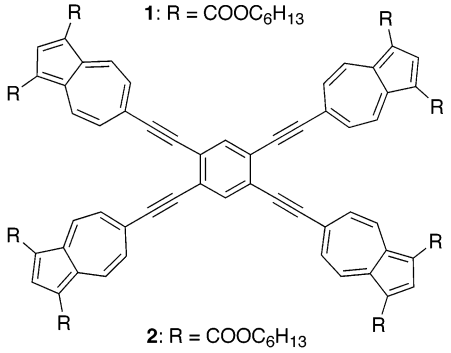

2: R = $COOC_6H_{13}$

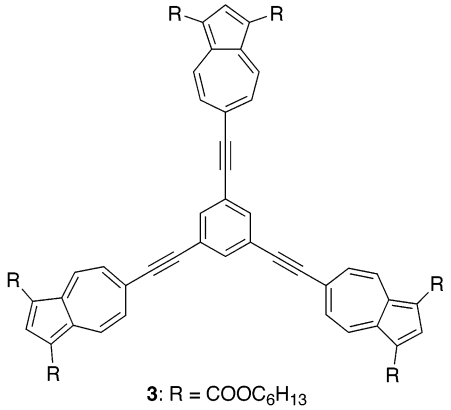

3: R = $COOC_6H_{13}$

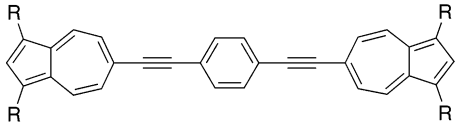

4a: R = COOEt
4b: R = $COOC_6H_{13}$

(6) Zeller, K.-P. Azulene. In *Houben-Weyl*; *Methoden der Organischen Chemie*; 4th ed.; Georg Thieme: Stuttgart, Germany, 1985; Vol. V, Part 2C, pp 127−418.
(7) (a) Kohne, B.; Praefcke, K. *Chimia* **1987**, *41*, 196−198. (b) Praefcke, K.; Kohne, B.; Singer, D.; Demus, D.; Pelzi, G.; Diele, S. *Liq. Cryst.* **1990**, *7*, 589−594. (c) Booth, C. J.; Krüerke, D.; Heppke, G. *J. Mater. Chem.* **1996**, *6*, 927−934.
(8) (a) Adam, D.; Schuhmacher, P.; Simmerer, J.; Häussling, L.; Siemensmeyer, K.; Etzbach, K. H.; Ringsdorf, H.; Haarer, D. *Nature* **1994**, *371*, 141−143. (b) Van de Craats, A. M.; De Haas, M. J.; Warman, J. M. *Synth. Met.* **1997**, *86*, 2125−2126. (c) Van de Craats, A. M.; Warman, J. M.; Hasebe, H.; Naito, R.; Ohta, K. *J. Phys. Chem. B* **1997**, *101*, 9224−9232. (d) Van de Craats, A. M.; Warman, J. M.; Müllen, K.; Geerts, Y.; Brand, J. D. *Adv. Mater.* **1998**, *10*, 36−38.
(9) (a) Nakamura, K.; Kaneko, S.; Ito, Y.; Hirabayashi, H.; Ogura, K. *J. Appl. Phys.* **1982**, *53*, 1792−1796. (b) Nakamura, K.; Nakada, K.; Ito, Y.; Koishi, E. *J. Appl. Phys.* **1983**, *57*, 135−140.
(10) Hafner et al. reported the ethynylation of azulenes in a five-membered ring utilizing Pd-catalyzed cross-coupling reaction and the preparation of benzene-bridged poly(1-alkynylazulene)s: (a) Fabian, K. H. H.; Elwahy, A. H. M.; Hafner, K. *Tetrahedron Lett.* **2000**, *41*, 2855−2858. (b) Elwahy, A. H. M.; Hafner, K. *Tetrahedron Lett.* **2000**, *41*, 2859−2862. (c) Elwahy, A. H. M.; Hafner, K. *Tetrahedron Lett.* **2000**, *41*, 4079−4083.

Scheme 2

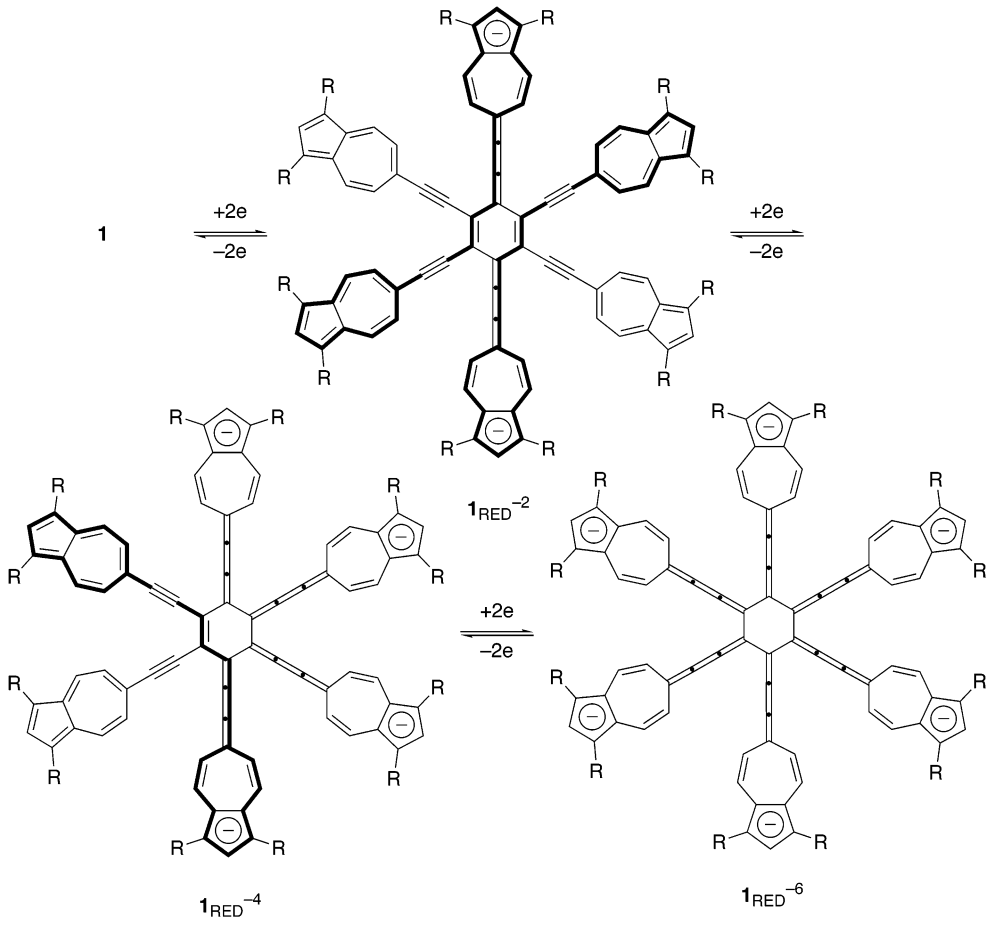

Scheme 3

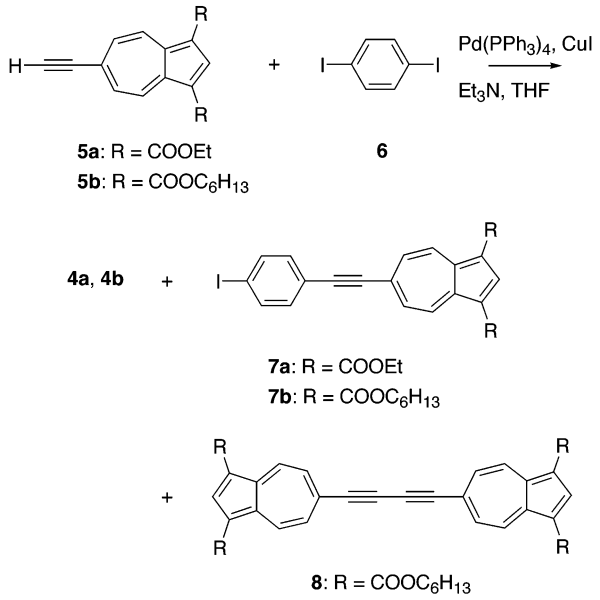

Scheme 4

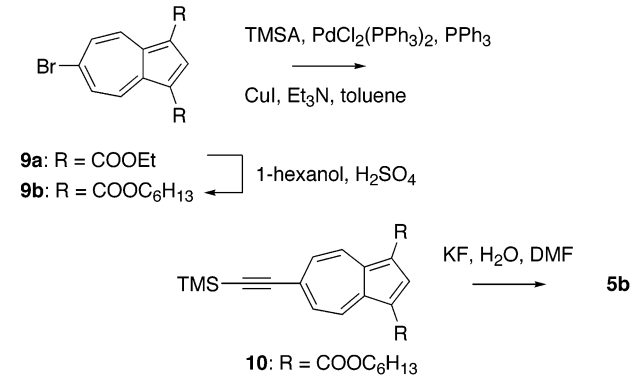

in 25% yield together with monoadduct **7a** in 12% yield (Scheme 3). However, the product **4a** exhibited fairly low solubility in common organic solvents. For this reason, poly(6-azulenylethynyl)benzenes substituted with hexyloxycarbonyl substituents at 1,3-positions in azulene rings were prepared by the coupling reaction.

Preparation of 6-ethynylazulene with hexyloxycarbonyl chains commenced with diethyl 6-bromoazulene dicarboxylate (**9a**)[12] was outlined in Scheme 4. The cross-coupling reaction of **5b** with 1,4-diiodobenzene (**6**) in the presence of Pd(0) catalyst afforded a mixture of bisadduct **4b** and monoadduct **7b** in 43% and 18% yields, respectively, together with diacetylene **8** in 16% yield (Scheme 4). Formation of **8** is presumably attributable to the low reactivity of **5b** with the aryl halide **6** under the cross-coupling conditions.[13] Likewise, the reaction of **9** with 1,2,4,5-

(11) (a) Sonogashira, K. *Comprehensive Organic Synthesis*; Trost, B. M., Fleming, I., Eds.; Pergamon Press: Oxford, U.K., 1991; Vol. 3, Chapt. 2.4, pp 521−549. (b) Takahashi, S.; Kuroyama, Y.; Sonogashira, K.; Hagihara, N. *Synthesis* **1980**, 627−630. (c) Sonogashira, K.; Tohda, Y.; Hagihara, N. *Tetrahedron Lett.* **1975**, 4467−4470.

(12) McDonald, R. N.; Richmond, J. M.; Curtis, J. R.; Petty, H. E.; Hoskins, T. L. *J. Org. Chem.* **1976**, *41*, 1811−1821.

(13) (a) Rossi, R.; Carpita, A.; Bigelli, C. *Tetrahedron Lett.* **1985**, *26*, 523−526. (b) Takahashi, A.; Endo, T.; Nozoe, S. *Chem. Pharm. Bull.* **1992**, *40*, 3181−3184.

Scheme 5

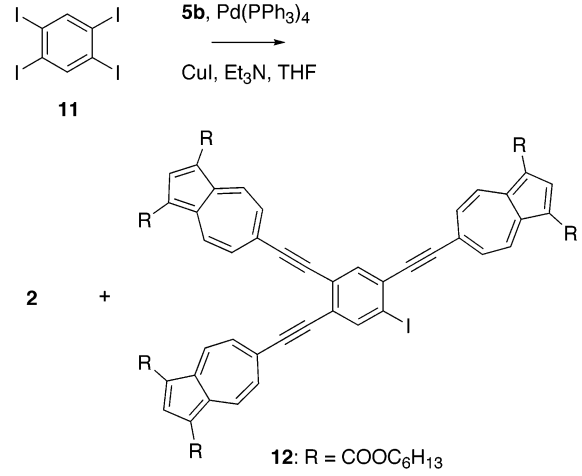

Scheme 6

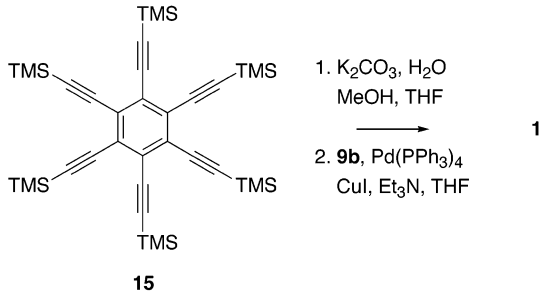

Scheme 7

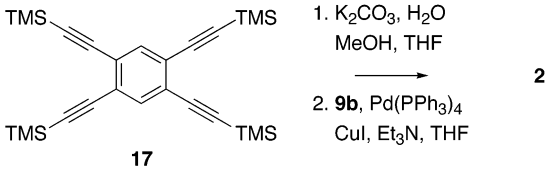

tetraiodobenzene (**11**)[14] gave **2** and **12** in 25% and 20% yields, respectively, together with **8** in 5% yield (Scheme 5). However, attempts made toward the 6-fold ethynylation of hexaiodobenzene (**13**) with **5b** did not afford the desired **1** even in a small amount.

The inverse cross-coupling reaction of dihexyl 6-bromoazulene-1,3-dicarboxylate (**9b**) with hexaethynylbenzene (**14**)[15] prepared in solution via hexakis(trimethylsilylethynyl)benzene (**15**) in the presence of Pd(0) catalyst afforded the desired **1** in 55% yield (Scheme 6). It is noteworthy that unstable **14** could be utilized in the 6-fold Sonogashira reaction without isolation. Compound **2** was also obtained by the reaction of **9b** with 1,2,4,5-tetraethynylbenzene (**16**)[16] generated in situ via 1,2,4,5-tetrakis(trimethylsilylethynyl)benzene (**17**) in 66% yield (Scheme 7). Likewise, the reaction of **9b** with 1,3,5-triethynylbenzene (**18**)[17] prepared from 1,3,5-tris(trimethylsilylethynyl)benzene (**19**) also afforded **3** in 96% yield (Scheme 8).

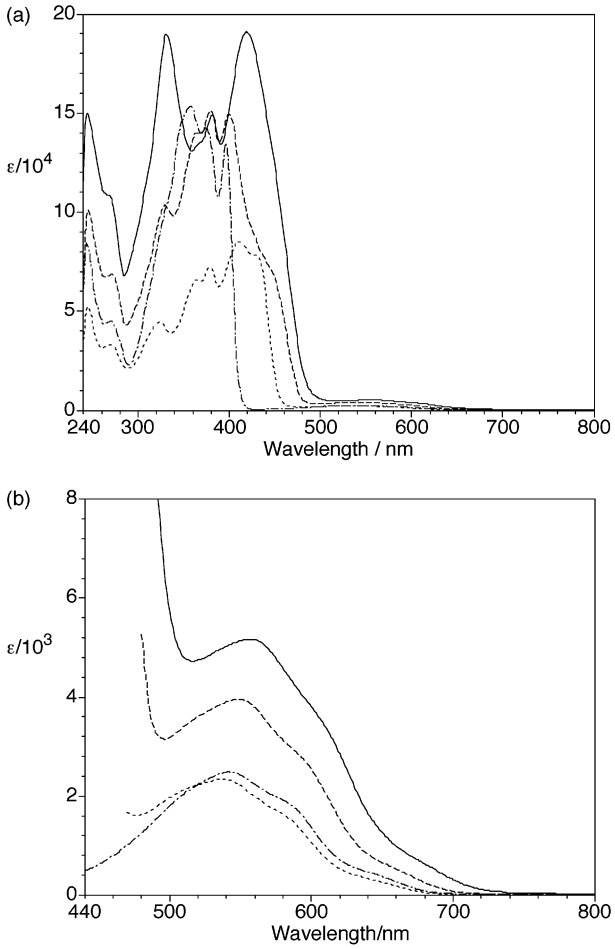

Figure 1. Spectra of **1** (—), **2** (---), **3** (···), and **4b** (— · —) in (a) UV−vis and (b) visible region in chloroform.

Scheme 8

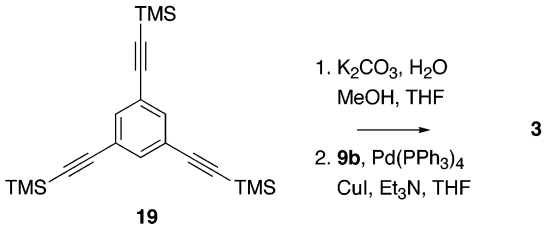

Poly(6-azulenylethynyl)benzenes substituted with *n*-hexyloxycarbonyl chains, **1**−**3** and **4b**, possess fair solubility in chloroform, dichloromethane, and so on. These compounds are stable, showing no decomposition even after several weeks at room temperature. The products **1**−**4** were fully characterized by the spectral data as shown in the Experimental Section. Mass spectra of **3** and **4b** ionized by FAB showed correct M^+ and $M^+ - OC_6H_{13}$ ion peaks, but higher molecular compounds could not be ionized by the method. Mass spectra of **1** and **2** were obtained by ESI-TOF MS, which exhibited the correct $M^+ +$ Na ion peak. UV−vis spectra of **1**−**3** and **4b** in chloroform are shown in Figure 1. They showed characteristic weak absorption of the azulene system in the visible region. The longest absorption maxima of **1**−**3** and **4b** in the visible region exhibited a slight bathochromic shift in the order of the number of azulene rings owing to the extension of the π-system.

Disc-type molecules have a tendency to form aggregates in solution, which causes significant line broadening and shielding

(14) Mattern, D. L. *J. Org. Chem.* **1984**, *49*, 3051−3053.
(15) Diercks, R.; Armstrong, J. C.; Boese, R.; Vollhart, K. P. C. *Angew. Chem., Int. Ed. Engl.* **1986**, *25*, 268−269.
(16) (a) Berris, B. C.; Hovakeemian, G. H.; Lai, Y.-H.; Mestdagh, H.; Vollhardt, K. P. C. *J. Am. Chem. Soc.* **1985**, *107*, 5670−5687. (b) Berris, B. C.; Hovakeemian, G. H.; Vollhart, K. P. C. *J. Chem. Soc., Chem. Commun.* **1983**, 502−503.
(17) (a) Osawa, M.; Sonoki, H.; Hoshino, M.; Wakatsuki, Y. *Chem. Lett.* **1998**, 1081−1082. (b) Anderson, H. L.; Walter, C. J.; Vidal-Ferran, A.; Hay, R. A.; Lowden, P. A. *J. Chem. Soc., Perkin Trans. 1* **1995**, 2275−2279. (c) Royles, B. J. L.; Smith, D. M. *J. Chem. Soc., Perkin Trans. 1* **1994**, 355−358.

Table 1. Reduction Potentials[a] of Compounds **1**−**3**, **4b**, and **12**

sample	E_1^{red}, V	E_2^{red}, V	E_3^{red}, V	E_4^{red}, V
1	(−1.28) (6e)			
2	−1.08 (2e)	−1.28 (2e)	(−2.05)	
12	−1.10 (2e)	(−1.28) (1e)	(−1.84)	(−1.98)
3	(−1.39) (3e)	(−2.10)		
4b	−1.19 (2e)	(−1.97)		

[a] The redox potentials were measured by cyclic voltammetry (CV) or differential pulse voltammetry (DPV) (0.1 M Bu_4NBF_4 in *o*-dichlorobenzene, Pt electrode, scan rate 100 mV/s^{-1}, and $Fc^+/Fc = 0.26$ V). In the case of irreversible waves, which are shown in parentheses, E_{ox} and E_{red} were calculated as E_{pa} (anodic peak potential) − 0.03 V and E_{pc} (cathodic peak potential) + 0.03 V, respectively.

in their NMR spectra.[18] Concentration dependence of the ^{1}H NMR spectrum of **1** exhibited some intermolecular aggregation in solution due to the $\pi-\pi$ interaction of aromatic cores. Increasing the concentration of **1** causes a high-field shift of the aromatic signals with considerable line broadening in the ^{1}H NMR spectra owing to the results in the larger aggregates formed.

Cyclic Voltammetry. Redox potentials (in volts vs Ag/Ag^+) of **1**−**3** and **4b** measured by cyclic voltammetry (CV) are summarized in Table 1. Compound **4b** showed a reversible two-electron transfer at −1.19 V upon CV (Figure 2d). The shape of CV does not exhibit real one-step, two-electron transfer. Therefore, the observed overall two-electron transfer in **4b** means the low semiquinone formation constant (K_{SEM}) in the redox system (Scheme 9). Similar one-step, two-electron reduction with a low K_{SEM} value has been observed in the 6,6′-biazulenyl separated by six methine groups.[19] The acetylenic and aromatic core in **4** would reduce coulomb repulsion further due to the larger distance of the charges.

Compound **3** exhibited an irreversible broad reduction wave, centered at around −1.39 V (Figure 2c). Compound **3** shows a potential gap of about 20 mV, which is less, as compared with that of **4b**, because the three 6-azulenylethynyl substituents on benzene in a 1,3,5 relationship cannot take a closed-shell dianionic structure like **4** as shown in Scheme 9.

In contrast to the one-step reduction of **3**, 1,2,4,5-tetrakis(6-azulenylethynyl)benzene **2** exhibited a barely separated two-step reduction wave at $E_{1/2} = -1.08$ and −1.28 V upon CV (Figure 2b). The electrochemical reduction of 1,2,4-tris(6-azulenylethynyl)-5-iodobenzene **12** exhibited a similar two-step reduction wave, but the wave was characterized by a two-electron reduction wave at −1.10 V and a one-electron transfer at −1.28 V. Therefore, the two waves observed by the reduction of **2** must correspond to the transfer of two electrons in both cases. Consequently, the redox system of **2** could be illustrated as a violene−cyanine hybrid and could exhibit a significant color change in a different oxidation state. The presumed cyanine-type structure formed by the two-electron reduction is represented by the bold line in Scheme 10.

Hexakis(6-azulenylethynyl)benzene (**1**) exhibited a quasi-reversible broad reduction wave, centered at around −1.28 V at the scan rate of 100 mV/s (Figure 2a). The wave was barely separated into two waves, at −1.12 and −1.23 V, by differential pulse voltammetry (DPV). We further extended the scan down to −2.5 V, but no other peaks were observed. Therefore, the

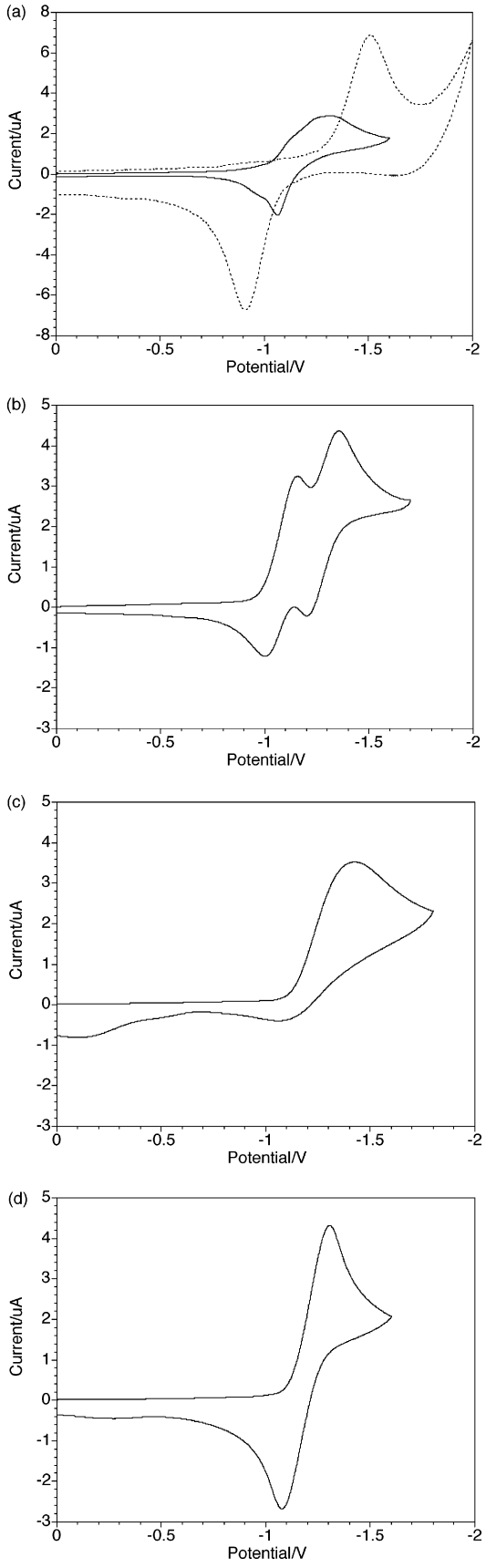

Figure 2. Cyclic voltammograms of (a) **1** (0.5 mM), (b) **2** (1 mM), (c) **3** (1 mM), and (d) **4b** (1 mM) in *o*-dichlorobenzene containing Bu_4NBF_4 (0.1 M) as a supporting electrolyte.

(18) Watson, M. D.; Fechtenkötter, A.; Müllen, K. *Chem. Rev.* **2001**, *101*, 1267−1300.
(19) Hünig, S.; Ort, B. *Liebigs Ann. Chem.* **1984**, 1959−1971.

Scheme 9

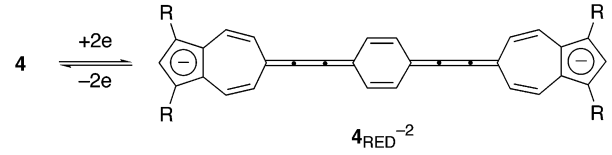

wave should be attributable to the six-electron transfer in one-step to generate a hexaanionic species $\mathbf{1}_{red}^{-6}$. Under the same conditions, with an increased scan rate, the peak separation is increased to $\Delta E = 599$ mV (500 mV/s). The scan rate dependence should be attributable to the conditions of the measurement because the peak separation of a ferrocenium/ferrocene (Fc^+/Fc) couple was also observed as 353 mV at a scan rate of 500 mV/s.

Electrochromic Behavior. UV−vis measurement of **1**−**3** and **4b** was examined to clarify the formation of a closed-shell cyanine-type structure under the electrochemical reduction conditions. A constant-current reduction was applied to the solutions of **1**−**3** and **4b**, with platinum wires for the working electrode and counterelectrode. When the UV−vis spectra of **1** and **2** were measured in *o*-dichlorobenzene containing Bu_4NBF_4 (0.1 M) at room temperature under the electrochemical reduction conditions, a new absorption in the visible region was gradually developed as shown in Figure 3. The color of the solution of **1** and **2** gradually changed from brown to black and pink, respectively, during the electrochemical reduction. Rather well-developed isosbestic points in the UV−vis spectra suggest the formation of a new species in solution. Thus, the color change of the solutions would be attributed to the formation of a cyanine-type structure in the two-electron reduction. However, the reverse oxidation of the colored solutions of **1** and **2** exhibited the bleaching of the color but not regeneration of the UV−vis spectra of the neutral **1** and **2**, although the reversibility was observed upon CV. These results indicate the low stability of the presumed anionic species under the conditions of the UV−vis measurement. Several acetylenes with pyridinyl end groups have been reported to afford extremely sensitive reduction products.[20] Therefore, the instability of the reduced species must be attributable to rapid polymerization of the cumulenes formed by the two-relectron reduction.

We also tried electrochemical reduction of **3** and **4b** under UV−vis monitoring, although these two compounds do not take a cyanine-type structure by the electrochemical reduction. In these cases, however, we could not obtain any evidence of the formation of a presumed radical anionic and/or dianionic species. Absence of the reversibility for the reduction of **3** and **4b** also suggests the instability of the presumed reduction products under the conditions of the UV−vis measurement.

Liquid-Crystalline Properties. Phase transition behavior of **1**−**3** and **4b** was examined with a polarizing microscope equipped with a heating plate controlled by a thermoregulator and measured with a differential scanning calorimeter (DSC). To distinguish between the solid polymorphs in the compounds, X-ray diffraction powder patterns were also measured with Cu Kα radiation. In Table 2 are summarized the phase transition temperatures and phase transition enthalpy changes for **1**−**3** and **4b**. The assignments of X-ray reflections of each of the mesophases are summarized in Table 3. The detailed thermal behaviors of these compounds are described below.

Compound **1** showed a very wide temperature range of columnar mesophases (Col_{ho} and Col_{ro}) from 77.3 °C to the decomposition temperature at ca. 270 °C. This is the first instance of the columnar mesophase in azulenic compounds.[21,22] When the virgin state of **1** [K(v) crystal phase] was heated at 77.3 °C, the K(v) phase transformed into a Col_{ho} mesophase. On further heating, the phase exhibited phase transition to a Col_{ro} (*C*2/*m*) mesophase. On further heating, the Col_{ro} phase decomposed at around 270 °C. We could not observe any texture changes between the Col_{ho} and Col_{ro} phases in **1** by microscopic observations owing to the high viscosity of these two mesophases. However, unequivocal characterization of each state was confirmed by X-ray diffraction experiments, which exhibited a diffuse band around $2\theta = 20°$ in the wide-angle region, corresponding to the melt of the hexyloxycarbonyl chains. The patterns revealed the columnar structures (Col_{ho} and Col_{ro}) of the two phases (Figure 4).

Compound **2** exhibited mesomorphism with crystalline polymorphs, K_1 and K_2. The solid obtained by the recrystallization (chloroform) of **2** was in amorphous state, which was revealed by X-ray diffraction experiments. When the virgin sample [amorphous solid (v)] was heated from room temperature, it crystallized gradually to afford K_1 crystals, which exhibited the solid−solid transition at 188.1 °C to give K_2 crystals. On further heating the sample to 215.0 °C, the K_2 crystals transformed into a columnar mesophase. The X-ray diffraction patterns of the mesophase at 230 °C are shown in Figure 5. The 13 narrow reflections in the low-angle region correspond to the columnar structure [Col_{ro} (*P*2/*a*)] of the mesophase with the lattice constants in a two-dimensional rectangular lattice, $a = 43.3$ Å, $b = 53.2$ Å. However, microscopic observations of the Col_{ro} phase in **2** also did not reveal any texture changes due to the high viscosity.

Compound **3** exhibited unusual multiple-melting behavior. Recrystallization of **3** (chloroform) afforded a crystalline phase, which was denoted as K_2(v). The double melting behavior of the K_2(v) phase was confirmed by DSC thermograms for all of the heating rates (1−40 °C/min) as shown in Figure 6. The two endothermic peaks II and IV on the thermograms correspond to the melting of K_2(v) and K_3 crystals, respectively. Exothermic peak III, between peaks II and IV, corresponds to the recrystallization from the melt of K_2 crystals to K_3 ones. The ratio of peak II [melting of K_2(v) phase] to peak IV (melting of K_3 phase) increases with faster heating rate. The solid−solid phase transition from K_2(v) to K_3 should correspond to peak I at around 60 °C.

The K_1 crystal phase including an unidentified X phase appeared on rapid cooling of an isotropic liquid heated over the melting point of the K_3 crystalline phase down to room temperature. The DSC thermograms of the rapid-cooled sample for different heating rates are shown in Figure 7. Endothermic peak I and exothermic peak II on the thermograms should correspond to the melting of the X phase and the recrystallization from the melt of the phase to K_1 crystals, respectively. Since the phase transition from K_1 to K_2 was observed by microscopic

(20) Hünig, S.; Berneth, H. *Top. Curr. Chem.* **1980**, *92*, 1−44.

(21) (a) Praefcke, K.; Schmidt, D. *Z. Naturforsch., B*: *Anorg. Chem., Org. Chem.* **1981**, *36B*, 375−378. (b) Estdale, S. E.; Brettle, R.; Dunmur, D. A.; Marson, C. M. *J. Mater. Chem.* **1997**, *7*, 391−401.

(22) (a) Morita, T.; Kaneko, M. Jpn. Pat. 03261745, 1991. (b) Morita, T.; Kaneko, M. Jpn. Pat. 03261754, 1991. (c) Morita, T.; Kaneko, M. Jpn. Pat. 03122189, 1991.

Scheme 10

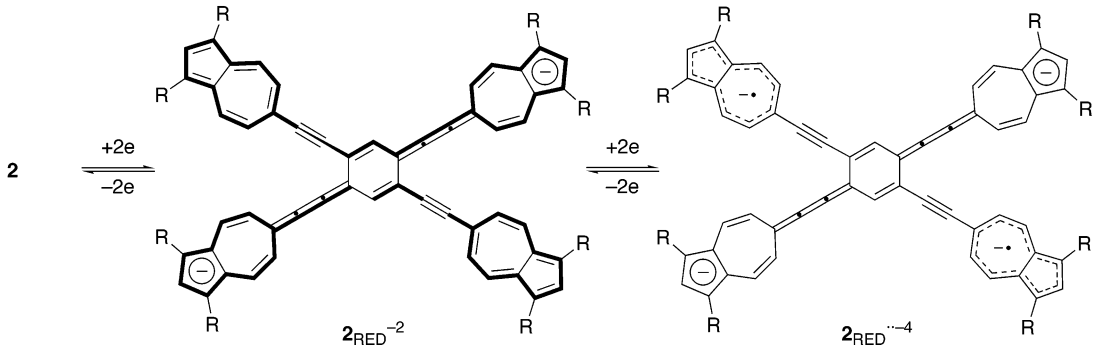

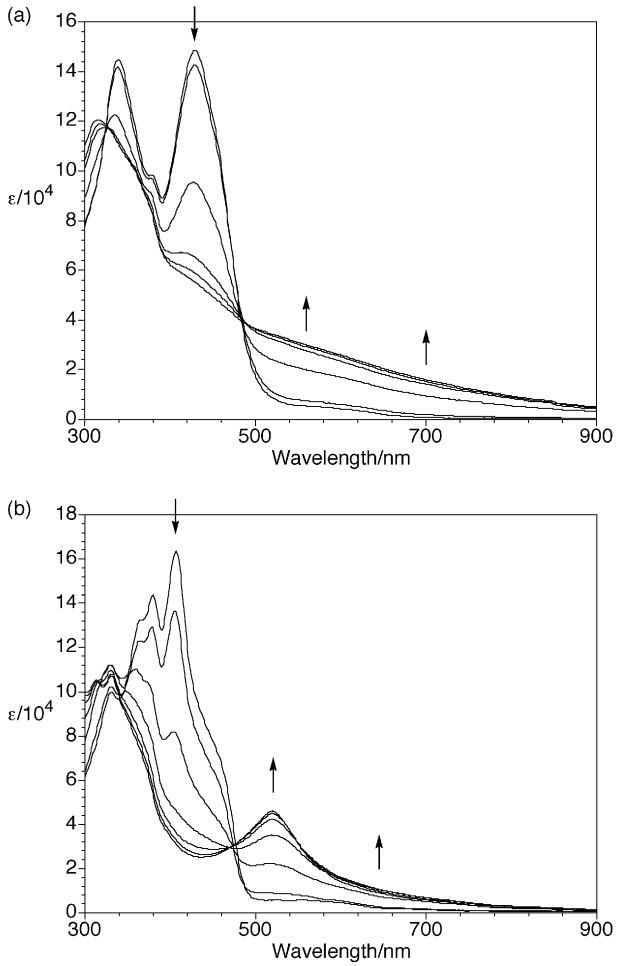

Figure 3. Continuous change in visible spectrum of (a) **1** (10 mL; 0.6×10^{-5} M) and (b) **2** (10 mL; 0.9×10^{-5} M) in *o*-dichlorobenzene containing Bu_4NBF_4 (0.1 M) upon constant-current electrochemical reduction (40 and 30 μA, respectively) at 10-min intervals.

observations, the exothermic peak II could include that of the phase transition. Endothermic peaks III and V on the thermograms correspond to the melting of K_1 and K_2 phases, respectively. Exothermic peak IV, between peaks III and V, corresponds to the recrystallization from the melt of K_1 crystals to K_2 ones. Consequently, the phase transition of **3** can be reasonably explained by using a Gibbs free energy versus temperature ($G-T$) diagram as shown in Figure 8.

Double melting behavior was observed for compound **4b**. Photomicrographs in Figure 9 show a sequence of the state changes for **4b**. Photo a shows the K_1(v) crystals obtained by recrystallization (chloroform) at 150.0 °C. Photo b exhibits the melt of K_1(v) crystals, when the sample in photo a was heated to 158.2 °C. The K_2 crystals were gradually solidified from the melt by holding the temperature at 158.2 °C for 30 min (photo c). The state change in photo c proceeded further by holding the temperature at 158.2 °C for 120 min (photo d). Photo e shows the growing of the K_2 crystals by holding the temperature at 158.2 °C for more than 480 min. When the sample in photo e was heated from 158.2 °C, the K_2 crystals started to melt at 161.2 °C (photo f). The K_2 crystals melted, completely, when the sample in photo e was heated to 162.0 °C (photo g).

Thus, the double melting behavior of compound **4b** was revealed by the polarizing microscopic observations. On the other hand, since the solid−solid phase transition from K_1(v) to K_2 and the relaxation of the melt of K_1(v) to K_2 are slow, the DSC measurements of the K_1(v) sample gave a single melting thermogram corresponding to the melting of the K_1(v) phase for any heating rate (1−10 °C/ min).

When the isotropic liquid of **4b** was cooled rapidly, the sample gave the mesophase, which showed a texture for the well-known developable units characteristic of columnar mesophases (Figure 10). The X-ray diffraction pattern of the mesophase at room temperature confirmed it as a hexagonal columnar structure (Col_{ho} phase) with the lattice constant $a = 34.9$ Å (Figure 11). Assuming a specific gravity of 1.2 g cm^{-3}, we can estimate the average number of molecules per unit cell as 3.1 molecules per 3.62 Å separation along the axis of the columns. This number of molecules per unit cell and the rodlike molecular shape are not typical for the 2D-hexagonal columnar system. Thus, the hexagonal symmetry of the mesophase of **4b** is rather unexpected.

The terms phasmid and phasmidic phase are proposed for the mesomorphic properties of molecules with a rodlike rigid core ending in two half-disk-shaped moieties.[23] The organization of **4b** may correspond to the stacking of the three rodlike molecules into a disk similar to the phasmidic phases. Thus, we can assume that the three molecules of **4b** form a cluster to arrange into a columnar mesophase according to a two-dimensional hexagonal lattice. The Col_{ho} phase showed relaxation to the K_2 phase at around 65 °C. However, the melting of the Col_{ho} phase could be detected at 148.3 °C by DSC and polarizing microscope heating the sample cooled to 135 °C from the isotropic liquid. Consequently, the schematic $G-T$ diagram of **4b** can be depicted as shown in Figure 12. The multiple-

(23) (a) Malthête, J.; Levelut, A. M.; Tinh, N. H. *J. Phys. Lett*. **1985**, *46*, 875−880. (b) Nguyen, H.-T.; Destrade, C.; Malthête, J. *Adv. Mater*. **1997**, *9*, 375−388.

Table 2. Phase Transition Temperature (T) and Enthalpy Changes (ΔH) of Compounds **1**−**3** and **4b**

compound	Phase[a] $\xrightarrow[[\Delta H^b\ (kJ/mol)]]{T^b\ (°C)}$ Phase ⇢ relaxation
1	K(v) $\xrightarrow[[118.7]]{77.3}$ Col_{ho} $\underset{[40.6]}{\overset{173.3}{\rightleftharpoons}}$ $Col_{ro}(C2/m)$ $\xrightarrow{ca.\ 270}$ decomp.
2	A.S.(v) ⇢ K_1 $\xrightarrow[[8.4]]{188.1}$ K_2 $\xrightarrow[[42.9]]{215.0}$ $Col_{ro}(P2/a)$ $\xrightarrow[[12.3]]{244.4}$ Y (decomp.)
3	X $\xrightarrow{120.7}$ I.L. ⇢ K_1 $\xrightarrow{139.0}$ I.L. ⇢ K_2(v) $\xrightarrow[[33.2]]{146.0}$ I.L. ⇢ K_3 $\xrightarrow{152.4}$ I.L. ⇢ X (ca. 120—130; ca. 60; rapid cooling)
4b	Col_{ho} $\xrightarrow{148.3}$ I.L. ⇢ K_1(v) $\xrightarrow[[68.8]]{158.1}$ I.L. ⇢ K_2 $\xrightarrow[[56.2]]{161.2}$ I.L. ⇢ Col_{ho} (ca. 65—100 [29.4]; ca. 109; rapid cooling)

[a] Phase nomenclature: K = crystal; Col_{ho} = discotic hexagonal columnar ordered mesophase; Col_{ro} = rectangular columnar odered mesophase; A.S. = amorphus solid; X, Y = unidentified phases; and I.L. = isotropic liquid. (v) Fresh virgin state obtained by recrystallization from solvent. [b] Phase transition temperature (T) and enthalpy change (ΔH) are determined by DSC.

melting behavior of **3** and **4b** is thought of as thermal behavior close to mesomorphism.[24]

Conclusions

Poly(6-azulenylethynyl)benzenes **1**−**4** substituted with *n*-hexyloxycarbonyl chains have been synthesized. Compounds **1**−**4** represented the presumed differences in the electron-transfer ability as a function of the relationship of the substituted positions. Compounds **1** and **2** exhibited color change under the electrochemical reduction. However, in the case of **1**, its electrochemical behavior was not ideal, probably due to the unfavorable steric interactions with two equal neighbors. With the systems **2**−**4**, all the electrochemical features could be verified, although not in an ideal way owing to the instability of the charged species. The poly(6-azulenylethynyl)benzenes **1**, **2**, and **4b** also showed columnar mesomorphism. The multiple-melting behavior was also observed in **2**, **3**, and **4b**. Thus, these system could be utilized to construct advanced materials for electrochromic application with liquid crystalline behavior.

Experimental Section

General Methods. For general experimental details and instrumentation, see our earlier publication.[25]

Dihexyl 6-Bromoazulene-1,3-dicarboxylate (9b). A solution of **9a** (5.00 g, 14.2 mmol), 1-hexanol (75.0 g, 734 mmol), and concentrated H_2SO_4 (4 mL) was stirred at 100 °C for 5 days. The reaction mixture was poured into water and extracted with toluene. The organic layer was washed with water, dried over $MgSO_4$, and concentrated. The residue was purified by column chromatography on silica gel with CH_2Cl_2 to afford **9b** (5.26 g, 80%) as red prisms: mp 115−117 °C (methanol); MS (70 eV) *m*/*z* (relative intensity) 464 ($M^+ + 2$, 100), 462 (M^+, 98), 361 ($M^+ - OC_6H_{13}$, 29), 294 ($M^+ - 2C_6H_{12}$, 45), 277 ($M^+ - OC_6H_{13} - C_6H_{12}$, 36); IR (KBr) ν_{max} 1678 (s, C=O) cm^{-1}; UV−vis ($CHCl_3$) λ_{max} 274 (log ϵ 4.33), 317 (4.79), 349 (3.94), 380 (3.95), 513 (2.77) nm; ^1H NMR (400 MHz, $CDCl_3$) δ = 9.49 (d, J = 11.3 Hz, 2H, $H_{4,8}$), 8.80 (s, 1H, H_2), 8.03 (d, J = 11.3 Hz, 2H, $H_{5,7}$), 4.37 (t, J = 6.7 Hz, 4H, $H_{1'}$), 1.82 (tt, J = 7.5, 6.7 Hz, 4H, $H_{2'}$), 1.49 (m, 4H, $H_{3'}$), 1.42−1.34 (m, 8H, $H_{4',5'}$), 0.92 (m, 6H, $H_{6'}$); ^{13}C NMR (100 MHz, $CDCl_3$) δ = 164.7 (CO), 143.6 (C_2), 142.2 ($C_{3a,8a}$), 138.5 (C_6), 137.2 ($C_{4,8}$), 133.7 ($C_{5,7}$), 117.9 ($C_{1,3}$), 64.5 ($C_{1'}$), 31.5 ($C_{4'}$), 28.8 ($C_{2'}$), 25.8 ($C_{3'}$), 22.5 ($C_{5'}$), 14.0 ($C_{6'}$). Anal. Calcd for $C_{24}H_{31}BrO_4$: C, 62.20; H, 6.74; Br, 17.24. Found: C, 62.12; H, 6.80; Br, 17.33.

Dihexyl 6-Trimethylsilylethynylazulene-1,3-dicarboxylate (10). TMSA (847 mg, 8.63 mmol) was added to a solution of **9b** (2.00 g, 4.32 mmol), PPh_3 (111 mg, 0.423 mmol), CuI (81 mg, 0.43 mmol), and $PdCl_2(PPh_3)_2$ (151 mg, 0.215 mmol) in triethylamine (26 mL) and toluene (95 mL). The resulting mixture was stirred at room temperature for 3 h under an Ar atmosphere. The reaction mixture was poured into 10% NH_4Cl solution and extracted with CH_2Cl_2. The organic layer was washed with water, dried over $MgSO_4$, and concentrated. The residue was purified by column chromatography on silica gel with 5% ethyl acetate/hexane to afford **10** (2.07 g, 100%) as purple needles: mp 83−85 °C (hexane); MS (70 eV) *m*/*z* (relative intensity) 480 (M^+, 100); IR (KBr) ν_{max} 2147 (m, C≡C), 1698 (s, C=O) cm^{-1}; UV−vis ($CHCl_3$) λ_{max} 277 (log ϵ 4.21), 330 (4.86), 360 (4.29), 368 (4.33), 537 (2.79) nm; ^1H NMR (400 MHz, $CDCl_3$) δ = 9.63 (d, J = 11.1 Hz, 2H, $H_{4,8}$),

(24) (a) Ohta, K.; Muroki, H.; Hatada, K.; Takagi, A.; Ema, H.; Yamamoto, I.; Matsuzaki, K. *Mol. Cryst. Liq. Cryst.* **1986**, *140*, 163−177. (b) Ohta, K.; Muroki, H.; Hatada, K.; Yamamoto, I.; Matsuzaki, K. *Mol. Cryst. Liq. Cryst.* **1985**, *130*, 249−263. (c) Ohta, K.; Takenaka, O.; Hasebe, H.; Morizumi, Y.; Fujimoto, T.; Yamamoto, I. *Mol. Cryst. Liq. Cryst.* **1991**, *195*, 103−121.
(25) Ito, S.; Okujima, T.; Morita, N. *J. Chem. Soc., Perkin Trans. 1* **2002**, 1896−1905.

Table 3. X-ray Diffraction Data of the Mesophase of **1**, **2**, and **4b**

lattice constant, Å	spacing, Å measured	spacing, Å calculated	Miller indices (*hkl*)
compound **1** (Col_{ho} at 165 °C)			
$a = 30.4$	25.7	26.4	(100)
$h = 3.53$	14.8	15.2	(110)
$Z = 1.0$ for $\rho^a = 1.50$	13.5	13.2	(200)
	8.79	8.79	(300)
	7.74	7.61	(220)
	6.77	6.59	(400)
	6.13	6.05	(320)
	4.72	4.73	(510)
	4.39	4.39	(600)
	ca. 4.2		b
	3.53		(001)
compound **1** [$Col_{ro}(C2/m)$ at 210 °C]			
$a = 56.2$	28.1	28.1	(200)
$b = 29.1$	25.8	25.8	(110)
$h = 3.77$	16.0	15.8	(310)
$Z = 2.0$ for $\rho^a = 1.35$	14.5	14.5	(020)
	13.1	12.9	(220)
	ca. 4.6		b
	3.77		(001)
compound **2** ($Col_{ro}(P2/a)$ at 230 °C)			
$a = 43.3$	26.6	26.6	(020)
$b = 53.2$	21.6	21.6	(200)
$h = 3.54$	19.5	20.0	(210)
$Z = 4.0$ for $\rho^a = 1.40$	15.0	14.4	(300)
	14.2	13.9	(310)
	13.5	13.3	(040)
	10.5	10.6	(410)
	8.91	8.86	(060)
	8.63	8.66	(500)
	7.82	7.78	(530)
	7.14	7.15	(610)
	6.67	6.68	(630)
	6.20	6.19	(560)
	ca. 4.5		b
	3.54		(001)
compound **4b** (Col_{ho} at room temp)			
$a = 34.9$	30.2	30.2	(100)
$h = 3.62$	17.6	17.5	(110)
$Z = 3.1$ for $\rho^a = 1.20$	15.2	15.1	(200)
	11.5	11.4	(210)
	10.1	10.1	(300)
	ca. 4.8		b
	3.62		(001)

[a] Assumed density (grams per cubic centimeter). [b] Halo of molten hexyloxycarbonyl chains.

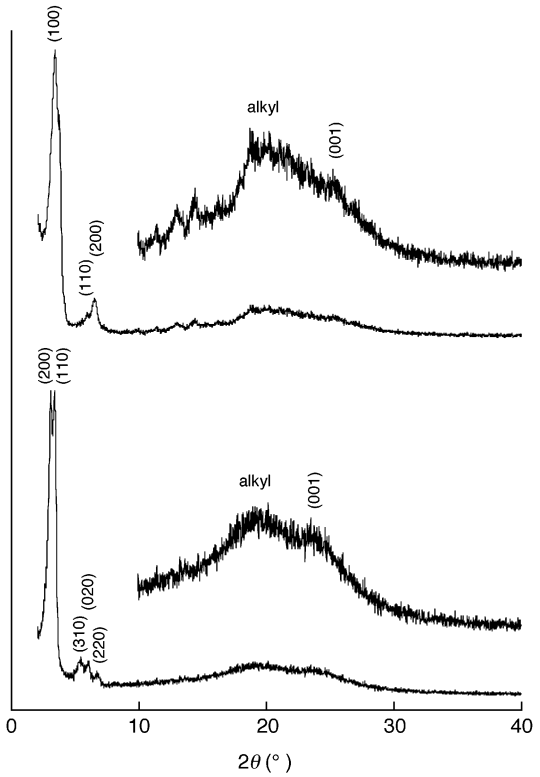

Figure 4. X-ray diffraction powder patterns of **1**: Col_{ho} mesophase at 165 °C (upper) and Col_{ro} ($C2/m$) mesophase at 210 °C (lower).

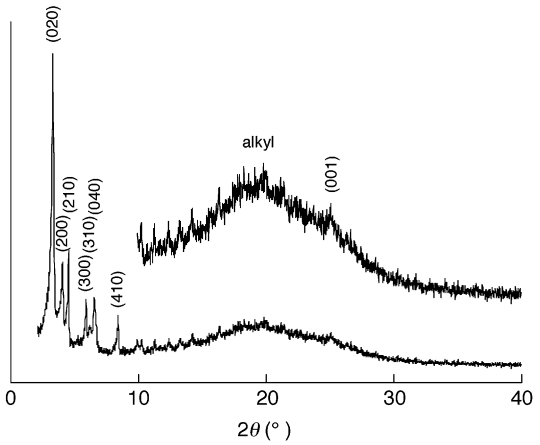

Figure 5. X-ray diffraction powder patterns of Col_{ro} ($P2/a$) mesophase for **2** at 230 °C.

8.77 (s, 1H, H_2), 7.84 (d, $J = 11.1$ Hz, 2H, $H_{5,7}$), 4.37 (t, $J = 6.9$ Hz, 4H, $H_{1''}$), 1.82 (tt, $J = 7.5$, 6.9 Hz, 4H, $H_{2''}$), 1.49 (m, 4H, $H_{3''}$), 1.42−1.34 (m, 8H, $H_{4'',5''}$), 0.92 (m, 6H, $H_{6''}$), 0.32 (s, 9H, 2′-TMS); ^{13}C NMR (100 MHz, $CDCl_3$) $\delta = 164.9$ (CO), 143.8 (C_2), 143.5 ($C_{3a,8a}$), 137.5 ($C_{4,8}$), 135.9 (C_6), 133.5 ($C_{5,7}$), 117.0 ($C_{1,3}$), 107.5 ($C_{1'}$), 101.3 ($C_{2'}$), 64.4 ($C_{1''}$), 31.5 ($C_{4''}$), 28.9 ($C_{2''}$), 25.8 ($C_{3''}$), 22.6 ($C_{5''}$), 14.0 ($C_{6''}$), −0.3 (2′-TMS). Anal. Calcd for $C_{29}H_{40}SiO_4$: C, 72.46; H, 8.39. Found: C, 71.86; H, 8.50.

Dihexyl 6-Ethynylazulene-1,3-dicarboxylate (5b). A solution of KF (184 mg, 3.17 mmol) in water (3 mL) was added to a solution of **10** (755 mg, 1.57 mmol) in DMF (35 mL). After the mixture was stirred at room temperature for 2 h, the reaction mixture was poured into water and extracted with toluene. The organic layer was washed with water, dried over $MgSO_4$, and concentrated to afford **5b** (617 mg, 96%) as purple needles: mp 118−119 °C (hexane); MS (70 eV) *m*/*z* (relative intensity) 408 (M^+, 100), 307 ($M^+ - OC_6H_{13}$, 26), 240 ($M^+ - 2C_6H_{12}$, 33), 223 ($M^+ - OC_6H_{13} - C_6H_{12}$, 35); IR (KBr) ν_{max} 3279 (m, C≡C−H), 2095 (m, C≡C), 1684 (s, C═O) cm^{-1}; UV−vis ($CHCl_3$) λ_{max} 276 (log ϵ 4.25), 322 (4.83), 346 (4.06), 354 (4.13), 379 (3.78), 538 (2.75) nm; ^{1}H NMR (400 MHz, $CDCl_3$) $\delta = 9.66$ (d, $J = 11.3$ Hz, 2H, $H_{4,8}$), 8.79 (s, 1H, H_2), 7.86 (d, $J = 11.3$ Hz, 2H, $H_{5,7}$), 4.37 (t, $J = 6.7$ Hz, 4H, $H_{1''}$), 3.48 (s, 1H, $H_{2'}$), 1.83 (tt, $J = 7.5$, 6.7 Hz, 4H, $H_{2''}$), 1.50 (m, 4H, $H_{3''}$), 1.42−1.34 (m, 8H, $H_{4'',5''}$), 0.92 (m, 6H, $H_{6''}$); ^{13}C NMR (100 MHz, $CDCl_3$) $\delta = 164.8$ (CO), 144.1 (C_2), 143.6 ($C_{3a,8a}$), 137.5 ($C_{4,8}$), 134.7 (C_6), 133.5 ($C_{5,7}$), 117.2 ($C_{1,3}$), 86.2 ($C_{1'}$), 82.3 ($C_{2'}$), 64.4 ($C_{1''}$), 31.5 ($C_{4''}$), 28.9 ($C_{2''}$), 25.8 ($C_{3''}$), 22.6 ($C_{5''}$), 14.0 ($C_{6''}$). Anal. Calcd for $C_{26}H_{32}O_4$: C, 76.44; H, 7.90. Found: C, 76.47; H, 8.02.

1,4-Bis[1,3-bis(hexyloxycarbonyl)-6-azulenylethynyl]benzene (4b). To a degassed solution of **5b** (311 mg, 0.761 mmol), **6** (100 mg, 0.303 mmol), CuI (2 mg, 0.01 mmol), and triethylamine (0.11 mL) in THF (15 mL) was added $Pd(PPh_3)_4$ (11 mg, 0.010 mmol). The resulting mixture was stirred at room temperature for 3 days under an Ar atmosphere. During the reaction period were added **5b** (309 mg, 0.756 mmol), CuI (24 mg, 0.13 mmol), and $Pd(PPh_3)_4$ (45 mg, 0.039 mmol), divided into several portions. The reaction mixture was diluted with CH_2Cl_2, washed successively with 5% NH_4Cl solution and brine, dried

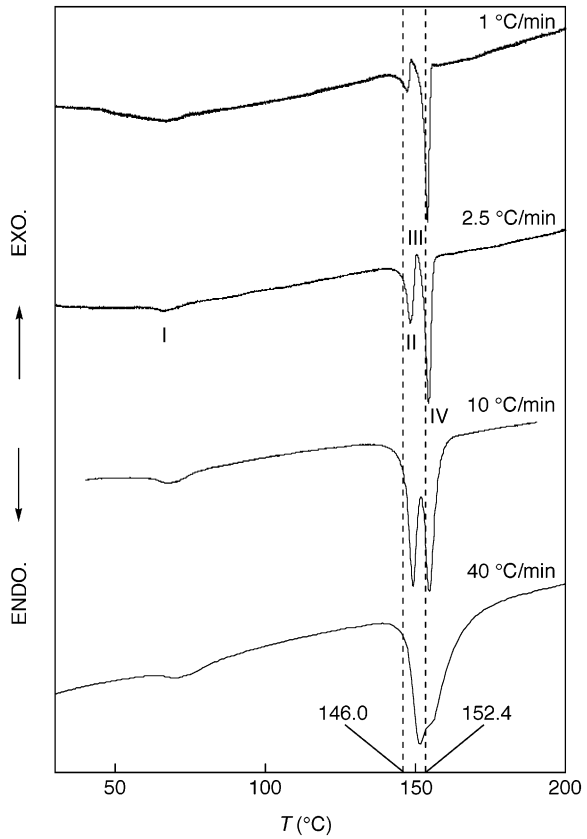

Figure 6. DSC thermograms of K_2(v) crystals of **3** for different heating rates. Peaks I−IV in the figure are explained in the main text.

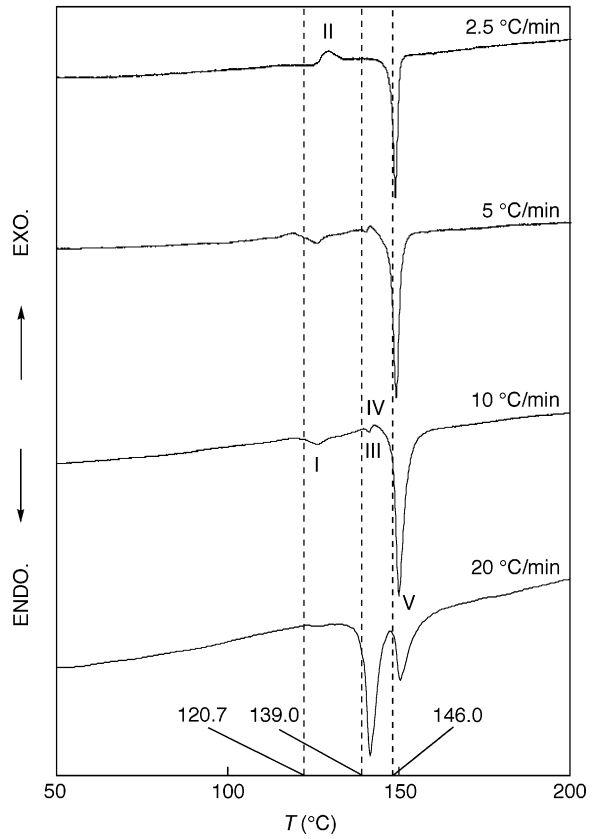

Figure 7. DSC thermograms of rapid-cooled sample of **3** for different heating rates. Peaks I−IV in the figure are explained in the main text.

over $MgSO_4$, and concentrated. The residue was purified by column chromatography on silica gel with CH_2Cl_2 and 5% ethyl acetate/CH_2Cl_2 and GPC with $CHCl_3$ to afford **4b** (117 mg, 43%) as brown crystals (ethyl acetate), **7b** (33 mg, 18%) as purple crystals, and **8** (99 mg, 16%) as green crystals.

4b: MS (FAB) *m*/*z* 891 ($M^+ + 1$), 890 (M^+), 789 ($M^+ - OC_6H_{13}$); IR (KBr) ν_{max} 2201 (m, C≡C), 1688 (s, C═O) cm^{-1}; UV−vis ($CHCl_3$) λ_{max} 270 (log ϵ 4.52), 324 (4.65), 364 (4.82), 379 (4.86), 411 (4.93), 428 (4.89), 538 (3.37) nm; ^{1}H NMR (500 MHz, $CDCl_3$) δ = 9.68 (d, J = 11.1 Hz, 4H, $H_{4'',8''}$), 8.78 (s, 2H, $H_{2''}$), 7.91 (d, J = 11.1 Hz, 4H, $H_{5'',7''}$), 7.65 (s, 4H, $H_{2,3,5,6}$), 4.38 (t, J = 6.7 Hz, 8H, $H_{1'''}$), 1.83 (tt, J = 7.6, 6.7 Hz, 8H, $H_{2'''}$), 1.50 (m, 8H, $H_{3'''}$), 1.41−1.35 (m, 16H, $H_{4''',5'''}$), 0.93 (m, 12H, $H_{6'''}$); ^{13}C NMR (125 MHz, $CDCl_3$) δ = 164.9 (CO), 143.8 ($C_{2''}$), 143.4 ($C_{3''a,8''a}$), 137.5 ($C_{4'',8''}$), 135.8 ($C_{6''}$), 133.1 ($C_{5'',7''}$), 132.2 ($C_{2,3,5,6}$), 128.1 ($C_{1,4}$), 117.2 ($C_{1'',3''}$), 95.1 ($C_{2'}$), 94.5 ($C_{1'}$), 64.4 ($C_{1'''}$), 31.5 ($C_{4'''}$), 28.9 ($C_{2'''}$), 25.8 ($C_{3'''}$), 22.6 ($C_{5'''}$), 14.0 ($C_{6'''}$). Anal. Calcd for $C_{58}H_{66}O_8$: C, 78.17; H, 7.46. Found: C, 78.15; H, 7.55.

7b: mp 123−125 °C; MS (70 eV) *m*/*z* (relative intensity) 610 (M^+, 6), 275 (100); IR (KBr) ν_{max} 2201 (m, C≡C), 1698 (s, C═O) cm^{-1}; UV−vis ($CHCl_3$) λ_{max} 357 (log ϵ 4.71), 374 (4.67), 398 (4.59), 539 (2.94) nm; ^{1}H NMR (500 MHz, $CDCl_3$) δ = 9.65 (d, J = 11.1 Hz, 2H, $H_{4',8'}$), 8.77 (s, 1H, $H_{2'}$), 7.87 (d, J = 11.1 Hz, 2H, $H_{5',7'}$), 7.75 (d, J = 8.5 Hz, 2H, $H_{3'',5''}$), 7.31 (d, J = 8.5 Hz, 2H, $H_{2'',6''}$), 4.37 (t, J = 6.7 Hz, 4H, $H_{1'''}$), 1.83 (tt, J = 7.6, 6.7 Hz, 4H, $H_{2'''}$), 1.50 (m, 4H, $H_{3'''}$), 1.41−1.34 (m, 8H, $H_{4''',5'''}$), 0.92 (m, 6H, $H_{6'''}$); ^{13}C NMR (125 MHz, $CDCl_3$) δ = 164.9 (CO), 143.7 ($C_{2'}$), 143.3 ($C_{3'a,8'a}$), 137.8 ($C_{3'',5''}$), 137.5 ($C_{4',8'}$), 135.9 ($C_{6'}$), 133.4 ($C_{2'',6''}$), 133.0 ($C_{5',7'}$), 121.5 ($C_{1''}$), 117.1 ($C_{1',3'}$), 95.9 ($C_{4''}$), 94.2 (C_2), 93.9 (C_1), 64.4 ($C_{1'''}$), 31.5 ($C_{4'''}$), 28.8 ($C_{2'''}$), 25.8 ($C_{3'''}$), 22.6 ($C_{5'''}$), 14.0 ($C_{6'''}$). HRMS calcd for $C_{32}H_{35}IO_4$ 610.1580, found 610.1578. Anal. Calcd for $C_{32}H_{35}IO_4$: C, 62.95; H, 5.78. Found: C, 62.90; H, 5.78.

8: mp 200−202 °C (ethyl acetate/hexane); MS (FAB) *m*/*z* 814 ($M^+ + 1$), 814 (M^+), 713 ($M^+ - OC_6H_{13}$); IR (KBr) ν_{max} 2139 (w, C≡C), 1692 (s, C═O) cm^{-1}; UV−vis ($CHCl_3$) λ_{max} 270 (log ϵ 4.46), 362 (4.85), 379 (4.86), 400 (4.79), 433 (4.85), 557 (3.28) nm; ^{1}H NMR (400 MHz, $CDCl_3$) δ = 9.66 (d, J = 10.2 Hz, 4H, $H_{4',8'}$), 8.80 (s, 2H, $H_{2'}$), 7.88 (d, J = 10.2 Hz, 4H, $H_{5',7'}$), 4.38 (t, J = 6.7 Hz, 8H, $H_{1''}$), 1.83 (tt, J = 7.6, 6.7 Hz, 8H, $H_{2''}$), 1.50 (m, 8H, $H_{3''}$), 1.42−1.34 (m, 16H, $H_{4'',5''}$), 0.93 (m, 12H, $H_{6''}$); ^{13}C NMR (100 MHz, $CDCl_3$) δ = 164.7 (CO), 144.6 ($C_{2'}$), 143.7 ($C_{3'a,8'a}$), 137.4 ($C_{4',8'}$), 133.7 ($C_{6'}$), 133.4 ($C_{5',7'}$), 117.7 ($C_{1',3'}$), 87.5 ($C_{1,4}$), 78.4 ($C_{2,3}$), 64.5 ($C_{1''}$), 31.5 ($C_{4''}$), 28.8 ($C_{2''}$), 25.8 ($C_{3''}$), 22.6 ($C_{5''}$), 14.0 ($C_{6''}$). Anal. Calcd for $C_{52}H_{62}O_8$: C, 76.63; H, 7.67. Found: C, 76.21; H, 7.59.

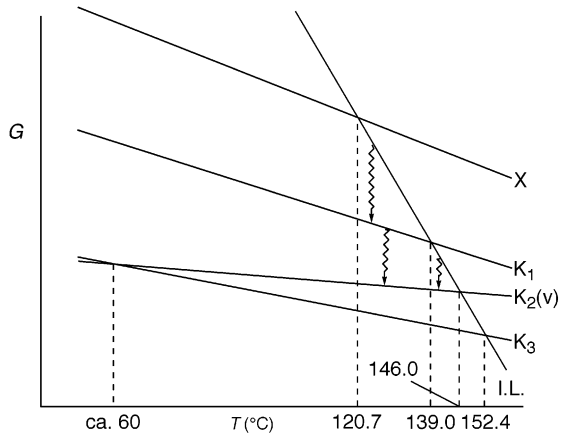

Figure 8. Schematic Gibbs free energy versus temperature ($G-T$) diagram of **3**.

1,4-Bis[1,3-bis(ethoxycarbonyl)-6-azulenylethynyl]benzene (4a). The same procedure as was used for the preparation of **4b** was adopted. The reaction of **5a** (90 mg, 0.30 mmol) with **6** (50 mg, 0.15 mmol) in triethylamine (10 mL) in the presence of $Pd(PPh_3)_4$ (17 mg, 0.015 mmol), PPh_3 (7 mg, 0.03 mmol), and CuI (6 mg, 0.03 mmol) at room

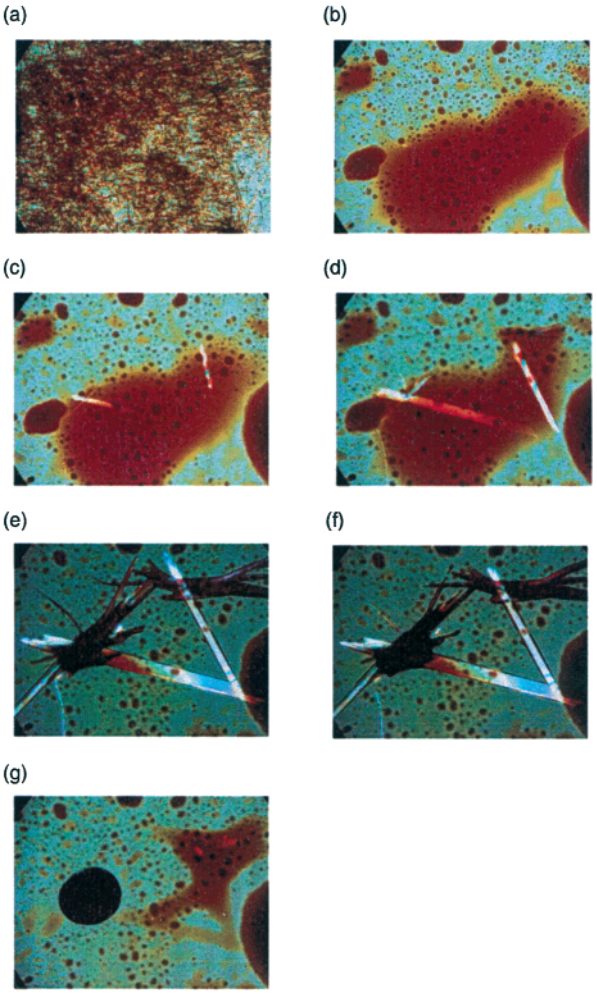

Figure 9. Photomicrographs of the double melting behavior of K_1 phase of **4b**: (a) at 150 °C, (b) at 158.2 °C, (c) at 158.2 °C after 30 min, (d) at 158.2 °C after 120 min, (e) at 158.2 °C after 480 min, (f) at 161.2 °C, and (g) at 162.0 °C.

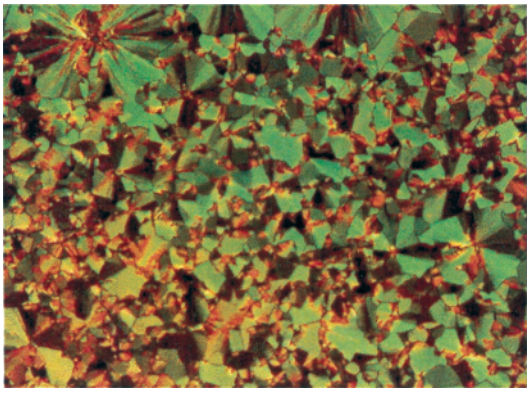

Figure 10. Texture of the discotic mesophase (Col_{ho}) of **4b** obtained by rapid cooling at room temperature.

temperature for 1 h followed by chromatographic purification on silica gel with 5% ethyl acetate/CH_2Cl_2 and GPC with $CHCl_3$ afforded **4a** (25 mg, 25%) as brown crystals and **7a** (9 mg, 12%) as purple crystals.

4a: mp 265.5−270 °C (ethyl acetate); MS (70 eV) *m*/*z* (relative intensity) 666 (M^+, 100); IR (KBr) ν_{max} 2201 (m, C≡C), 1694 (s, C═O) cm^{-1}; UV−vis ($CHCl_3$) λ_{max} 270 (log ϵ 4.49), 325 (4.59), 364 (4.74), 378 (4.78), 410 (4.83), 429 (4.80), 535 (3.27) nm; ^{1}H NMR (500 MHz, $CDCl_3$) δ = 9.70 (d, J = 11.1 Hz, 4H, $H_{4'',8''}$), 8.81 (s, 2H, $H_{2''}$), 7.93 (d, J = 11.1 Hz, 4H, $H_{5'',7''}$), 7.67 (s, 4H, $H_{2,3,5,6}$), 4.45 (q, J = 7.1 Hz, 8H, 1″,3″-COOEt), 1.47 (t, J = 7.1 Hz, 12H, 1″,3″-COOEt); ^{13}C NMR (125 MHz, $CDCl_3$) δ = 164.9 (s, 1″,3″-COOEt), 143.9 ($C_{2''}$), 143.5 ($C_{3''a,8''a}$), 137.6 ($C_{4'',8''}$), 135.9 ($C_{6''}$), 133.2 ($C_{5'',7''}$), 132.3 ($C_{2,3,5,6}$), 123.1 ($C_{1,4}$), 117.2 ($C_{1',3'}$), 95.1 ($C_{2'}$), 94.5 ($C_{1'}$), 60.2 (t, 1″,3″-COOEt), 14.6 (q, 1″,3″-COOEt). HRMS calcd for $C_{42}H_{34}O_8$ 666.2254, found 666.2236. Anal. Calcd for $C_{42}H_{34}O_8 \cdot H_2O$: C, 73.67; H, 5.30. Found: C, 73.19; H, 5.18.

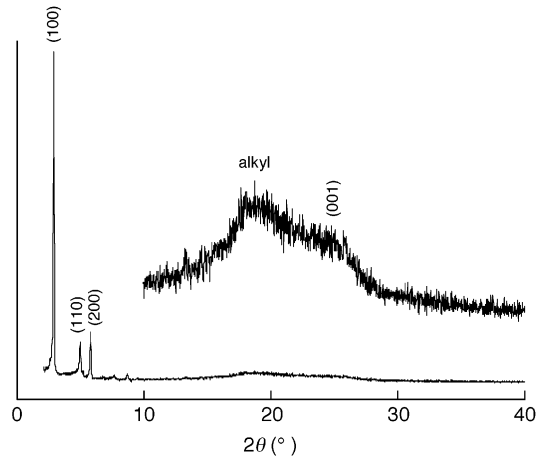

Figure 11. X-ray diffraction powder patterns of **4b** (Col_{ho} mesophase obtained by rapid cooling at room temperature).

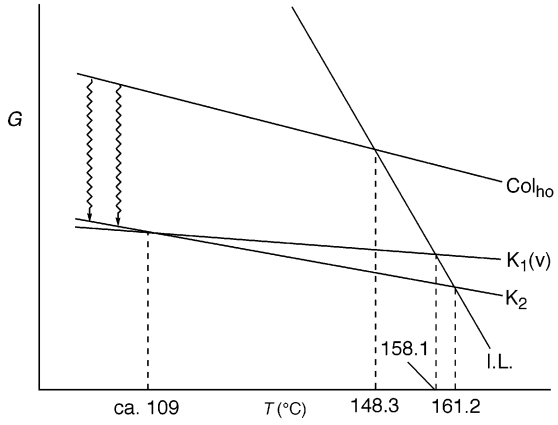

Figure 12. Schematic Gibbs free energy versus temperature ($G-T$) diagram of **4b**.

7a: mp 155−160 °C; MS (70 eV) *m*/*z* (relative intensity) 498 (M^+, 100), 453 (M^+ − OEt, 23); IR (KBr) ν_{max} 2201 (m, C≡C), 1684 (s, C═O) cm^{-1}; UV−vis ($CHCl_3$) λ_{max} 328 (log ϵ 4.51), 357 (4.66), 374 (4.62), 398 (4.54), 537 (2.93) nm; ^{1}H NMR (500 MHz, $CDCl_3$) δ = 9.67 (d, J = 11.2 Hz, 2H, $H_{4',8'}$), 8.80 (s, 1H, $H_{2'}$), 7.89 (d, J = 11.2 Hz, 2H, $H_{5',7'}$), 7.76 (d, J = 8.2 Hz, 2H, $H_{3'',5''}$), 7.33 (d, J = 8.2 Hz, 2H, $H_{2'',6''}$), 4.44 (q, J = 7.1 Hz, 4H, 1′,3′-COOEt), 1.46 (t, J = 7.1 Hz, 6H, 1′,3′-COOEt); ^{13}C NMR (125 MHz, $CDCl_3$) δ = 164.9 (s, 1′,3′-COOEt), 143.8 ($C_{2'}$), 143.4 ($C_{3'a,8'a}$), 137.8 ($C_{3'',5''}$), 137.5 ($C_{4',8'}$), 136.0 ($C_{6'}$), 133.4 ($C_{2'',6''}$), 133.1 ($C_{5',7'}$), 121.5 ($C_{1''}$), 117.1 ($C_{1',3'}$), 95.9 (C_2 or $C_{4''}$), 94.2 (C_2 or $C_{4''}$), 93.9 (C_1), 60.2 (t, 1′,3′-COOEt), 14.5 (q, 1′,3′-COOEt). HRMS calcd for $C_{24}H_{19}IO_4$ 498.0328, found 498.0339. Anal. Calcd for $C_{24}H_{19}IO_4 \cdot 0.5H_2O$: C, 56.82; H, 3.97. Found: C, 56.58; H, 3.91.

Hexakis[1,3-bis(hexyloxycarbonyl)-6-azulenylethynyl]benzene (1). To a degassed solution of **15** (101 mg, 0.154 mmol) in water (0.2 mL), THF (11 mL), and methanol (15 mL) was added K_2CO_3 (16 mg, 0.12 mmol). The resulting mixture was stirred at room temperature for 100 min. After an addition of water and diethyl ether to the reaction mixture, the organic layer was separated, washed with water, dried over $MgSO_4$, and concentrated to 5 mL. The residue was diluted with THF (5 mL), and triethylamine (1 mL), **9b** (500 mg, 1.08 mmol), and CuI (3 mg,

0.02 mmol) were added to the solution. After an addition of $Pd(PPh_3)_4$ (9 mg, 0.008 mmol) to the degassed mixture, the mixture was stirred at room temperature for 21 h and then refluxed for 18 h. The reaction mixture was diluted with $CHCl_3$, washed successively with 10% NH_4Cl solution and brine, dried over $MgSO_4$, and concentrated. The residue was purified by column chromatography on silica gel with $CHCl_3$ and 10% ethyl acetate/$CHCl_3$ to afford **1** (214 mg, 55%) as brown crystals (chloroform): MS (ESI-TOF) *m*/*z* 2540.24 ($M^+ + Na$) [calcd 2539.33]; IR (KBr) ν_{max} 1694 (s, C═O) cm^{-1}; UV−vis ($CHCl_3$) λ_{max} 331 (log ϵ 5.28), 381 (5.17), 419 (5.28), 558 (3.71) nm; ^1H NMR (500 MHz, $CDCl_3$) δ = 9.58 (d, J = 10.9 Hz, 12H, $H_{4'',8''}$), 8.67 (s, 6H, $H_{2''}$), 7.97 (d, J = 10.9 Hz, 12H, $H_{5'',7''}$), 4.33 (t, J = 6.9 Hz, 24H, $H_{1'''}$), 1.77 (tt, J = 7.6, 6.9 Hz, 24H, $H_{2'''}$), 1.45 (m, 24H, $H_{3'''}$), 1.36−1.30 (m, 48H, $H_{4''',5'''}$), 0.90 (m, 36H, $H_{6'''}$); ^{13}C NMR (125 MHz, $CDCl_3$) δ = 164.3 (CO), 144.6 ($C_{2''}$), 143.4 ($C_{3''a,8''a}$), 137.6 ($C_{4'',8''}$), 133.9 ($C_{6''}$), 132.5 ($C_{5'',7''}$), 128.5 ($C_{1,2,3,4,5,6}$), 118.1 ($C_{1'',3''}$), 104.5 ($C_{2'}$), 90.6 ($C_{1'}$), 64.4 ($C_{1'''}$), 31.6 ($C_{4'''}$), 28.9 ($C_{2'''}$), 25.9 ($C_{3'''}$), 22.6 ($C_{5'''}$), 13.9 ($C_{6'''}$). Anal. Calcd for $C_{162}H_{186}O_{24}$: C, 77.30; H, 7.45. Found: C, 77.19; H, 7.81.

1,2,4,5-Tetrakis[1,3-bis(hexyloxycarbonyl)-6-azulenylethynyl]benzene (2): Method 1. The same procedure as was used for the preparation of **1** was adopted. Compound **16** was prepared by the desilylation of **17** (100 mg, 0.216 mmol) by K_2CO_3 (21 mg, 0.15 mmol) in water (0.1 mL), THF (5 mL), and methanol (15 mL). The reaction of **9b** (499 mg, 1.08 mmol) with **16** in triethylamine (1 mL) and THF (10 mL) in the presence of $Pd(PPh_3)_4$ (12 mg, 0.010 mmol) and CuI (4 mg, 0.02 mmol) at room temperature for 15 h, followed by chromatographic purification on silica gel with $CHCl_3$ and 10% ethyl acetate/$CHCl_3$, afforded **2** (244 mg, 66%) as brown crystals (chloroform).

Method 2. The same procedure as was used for the preparation of **4b** was adopted. Compound **5b** (178 mg, 0.436 mmol) was reacted with **11** (50 mg, 0.086 mmol) in triethylamine (0.06 mL) and THF (5 mL) in the presence of $Pd(PPh_3)_4$ (4 mg, 0.003 mmol) and CuI (0.4 mg, 0.002 mmol), at room temperature for 22 h. During the reaction period were added **5b** (180 mg, 0.441 mmol) and $Pd(PPh_3)_4$ (3 mg, 0.003 mmol). Chromatographic purification of the reaction mixture on silica gel with CH_2Cl_2 and 10% ethyl acetate/CH_2Cl_2 and GPC with $CHCl_3$ afforded **2** (37 mg, 25%), **12** (25 mg, 20%) as brown crystals, and **8** (17 mg, 5%).

2: MS (ESI-TOF) *m*/*z* 1726.95 ($M^+ + Na$) [calcd 1726.90]; IR (KBr) ν_{max} 2203 (w, C≡C), 1692 (s, C═O) cm^{-1}; UV−vis ($CHCl_3$) λ_{max} 271 (log ϵ 4.84), 329 (5.01), 365 (5.15), 379 (5.18), 399 (5.17), 548 (3.60) nm; ^1H NMR (500 MHz, $CDCl_3$) δ = 9.65 (d, J = 10.9 Hz, 8H, $H_{4'',8''}$), 8.74 (s, 4H, $H_{2''}$), 8.00 (s, 2H, $H_{3,6}$), 7.93 (d, J = 10.9 Hz, 8H, $H_{5'',7''}$), 4.37 (t, J = 6.8 Hz, 16H, $H_{1'''}$), 1.81 (tt, J = 7.9, 6.8 Hz, 16H, $H_{2'''}$), 1.48 (m, 16H, $H_{3'''}$), 1.38−1.35 (m, 32H, $H_{4''',5'''}$), 0.91 (m, 24H, $H_{6'''}$); ^{13}C NMR (125 MHz, $CDCl_3$) δ = 164.7 (CO), 144.3 ($C_{2''}$), 143.4 ($C_{3''a,8''a}$), 137.5 ($C_{4'',8''}$), 136.5 ($C_{3,6}$), 134.7 ($C_{6''}$), 132.8 ($C_{5'',7''}$), 125.7 ($C_{1,2,4,5}$), 117.6 ($C_{1'',3''}$), 99.8 ($C_{2'}$), 91.5 ($C_{1'}$), 64.5 ($C_{1'''}$), 31.5 ($C_{4'''}$), 28.9 ($C_{2'''}$), 25.8 ($C_{3'''}$), 22.6 ($C_{5'''}$), 14.0 ($C_{6'''}$). Anal. Calcd for $C_{110}H_{126}O_{16}$: C, 77.53; H, 7.45. Found: C, 77.31; H, 7.51.

12: mp 200−202 °C (toluene); MS (ESI-TOF) *m*/*z* 1445.58 ($M^+ + Na$) [calcd 1445.58]; IR (KBr) ν_{max} 2201 (w, C≡C), 1694 (s, C═O) cm^{-1}; UV−vis ($CHCl_3$) λ_{max} 270 (log ϵ 4.71), 326 (4.92), 361 (5.04), 378 (5.06), 546 (3.45) nm; ^1H NMR (500 MHz, $CDCl_3$) δ = 9.70 (d, J = 11.1 Hz, 2H, $H_{4'',8''}$), 9.67 (d, J = 11.1 Hz, 4H, $H_{4'',8''}$), 8.79 (s, 3H, $H_{2''}$), 8.23 (s, 1H, H_6), 7.96 (d, J = 11.1 Hz, 2H, $H_{5'',7''}$), 7.94 (d, J = 11.1 Hz, 2H, $H_{5'',7''}$), 7.92 (d, J = 11.1 Hz, 2H, $H_{5'',7''}$), 7.86 (s, 1H, H_3), 4.38 (t, J = 6.8 Hz, 4H, $H_{1'''}$), 4.36 (t, J = 6.8 Hz, 8H, $H_{1'''}$), 1.86−1.77 (m, 12H, $H_{2'''}$), 1.52−1.45 (m, 12H, $H_{3'''}$), 1.39−1.34 (m, 12H, $H_{4''',5'''}$), 0.95−0.89 (m, 18H, $H_{6'''}$); ^{13}C NMR (125 MHz, $CDCl_3$) δ = 164.8 (CO), 164.7 (CO), 144.4 ($C_{2''}$), 144.3 ($C_{2''}$), 143.5 ($C_{3''a,8''a}$), 142.5 (C_6), 137.6 ($C_{4'',8''}$), 135.8 (C_3), 134.9 ($C_{6''}$), 134.8 ($C_{6''}$), 134.7 ($C_{6''}$), 132.9 ($C_{5'',7''}$), 132.8 ($C_{5'',7''}$), 129.8 (C_2 or C_4), 126.3 (C_5), 125.0 (C_2 or C_4), 117.6 ($C_{1'',3''}$), 117.4 ($C_{1'',3''}$), 101.8 (C_1), 100.0 ($C_{2'}$), 98.6 ($C_{2'}$), 95.4 ($C_{1'}$), 91.2 ($C_{1'}$), 90.9 ($C_{1'}$), 64.5 ($C_{1'''}$), 31.5 ($C_{4'''}$), 28.9 ($C_{2'''}$), 28.8 ($C_{2'''}$), 25.8 ($C_{3'''}$), 22.6 ($C_{5'''}$), 14.0 ($C_{6'''}$). Anal. Calcd for $C_{84}H_{95}IO_{12}$: C, 70.87; H, 6.73. Found: C, 70.70; H, 6.93.

1,3,5-Tris[1,3-bis(hexyloxycarbonyl)-6-azulenylethynyl]benzene (3). The same procedure as was used for the preparation of **1** was adopted. Compound **18** was prepared by the desilylation of **19** (100 mg, 0.273 mmol) by K_2CO_3 (26 mg, 0.19 mmol) in water (0.25 mL), THF (40 mL), and methanol (13 mL). The reaction of **9b** (503 mg, 1.09 mmol) with **18** in triethylamine (1 mL) and THF (10 mL) in the presence of $Pd(PPh_3)_4$ (15 mg, 0.013 mmol) and CuI (6 mg, 0.03 mmol) at room temperature for 15 h, followed by chromatographic purification on silica gel with $CHCl_3$ and 5% ethyl acetate/$CHCl_3$, afforded **3** (340 mg, 96%) as purple crystals (ethyl acetate): MS (FAB) *m*/*z* 1298 ($M^+ + 1$), 1297 (M^+), 1196 ($M^+ - OC_6H_{13}$); IR (KBr) ν_{max} 2203 (m, C≡C), 1698 (s, C═O) cm^{-1}; UV−vis ($CHCl_3$) λ_{max} 270 (log ϵ 4.65), 357 (5.18), 374 (5.15), 396 (5.13), 542 (3.40) nm; ^1H NMR (500 MHz, $CDCl_3$) δ = 9.60 (d, J = 11.1 Hz, 6H, $H_{4'',8''}$), 8.71 (s, 3H, $H_{2''}$), 7.84 (d, J = 11.1 Hz, 6H, $H_{5'',7''}$), 7.82 (s, 3H, $H_{2,4,6}$), 4.37 (t, J = 6.8 Hz, 12H, $H_{1'''}$), 1.84 (tt, J = 7.9, 6.8 Hz, 12H, $H_{2'''}$), 1.51 (m, 12H, $H_{3'''}$), 1.42−1.36 (m, 24H, $H_{4''',5'''}$), 0.94 (m, 18H, $H_{6'''}$); ^{13}C NMR (125 MHz, $CDCl_3$) δ = 164.7 (CO), 143.9 ($C_{2''}$), 143.3 ($C_{3''a,8''a}$), 137.4 ($C_{4'',8''}$), 135.6 ($C_{2,4,6}$), 135.1 ($C_{6''}$), 132.9 ($C_{5'',7''}$), 123.5 ($C_{1,3,5}$), 117.2 ($C_{1'',3''}$), 94.4 ($C_{2'}$), 92.3 ($C_{1'}$), 64.4 ($C_{1'''}$), 31.5 ($C_{4'''}$), 28.9 ($C_{2'''}$), 25.8 ($C_{3'''}$), 22.6 ($C_{5'''}$), 14.0 ($C_{6'''}$). Anal. Calcd for $C_{84}H_{96}O_{12}$: C, 77.75; H, 7.46. Found: C, 77.71; H, 7.54.

Acknowledgment. We are grateful to Professor Nagao Kobayashi and Dr. Kazuyuki Ishii of Tohoku University for the measurement of ESI-TOF MS.

JA0209262